

MICROCOPY RESOLUTION TEST CHART
NATIONAL BUREAU OF STANDARDS 1963 A

AD A089614

DDC FILE COPY

THE AEROSPACE CORPORATION

SPACE DIVISION

AIR FORCE SYSTEMS COMMAND

Los Angeles Air Force Station

P.O. Box 92960, Worldway Postal Center

Los Angeles, Calif. 90009

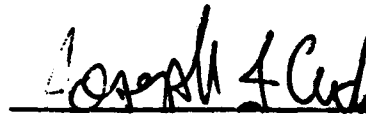
80 9 26 021

This interim report was submitted by The Aerospace Corporation, El Segundo, CA 90245, under Contract No. F04701-79-C-0080 with the Space Division, Deputy for Technology, P.O. Box 92960, Worldway Postal Center, Los Angeles, CA 90009. It was reviewed and approved for The Aerospace Corporation by W. R. Warren, Jr., Director, Aerophysics Laboratory. Lieutenant J. C. Garcia, SD/YLXT, was the project officer for Technology.

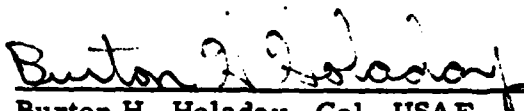
This report has been reviewed by the Public Affairs Office (PAS) and is releasable to the National Technical Information Service (NTIS). At NTIS, it will be available to the general public, including foreign nations.

This technical report has been reviewed and is approved for publication. Publication of this report does not constitute Air Force approval of the report's findings or conclusions. It is published only for the exchange and stimulation of ideas.


James C. Garcia, Lt, USAF
Project Officer


Joseph J. Cox, Jr., LtCol, USAF
Chief, Advanced Technology
Division

FOR THE COMMANDER


Burton H. Holaday, Col, USAF
Director of Space Systems Planning
Deputy for Technology

UNCLASSIFIED

SECURITY CLASSIFICATION OF THIS PAGE (When Data Entered)

19 REPORT DOCUMENTATION PAGE		READ INSTRUCTIONS BEFORE COMPLETING FORM
1. REPORT NUMBER SD TR-80-51	2. GOVT ACCESSION NO. AD-A089614	3. RECIPIENT'S CATALOG NUMBER
4. TITLE (and Subtitle) EXPERIMENTAL STUDIES OF ANNULAR (HSURIA) RESONATORS INCLUDING POLARIZATION EFFECTS.	5. TYPE OF REPORT & PERIOD COVERED 9 Interim rpt.	6. PERFORMING ORG. REPORT NUMBER 14 TR-0080(5605)-1
7. AUTHOR(s) 10 R. A. Chodsko / S. B. Mason and E. B. Turner	8. CONTRACT OR GRANT NUMBER(s) 15 F04701-79-C-0080	10. PROGRAM ELEMENT, PROJECT, TASK AREA & WORK UNIT NUMBERS
9. PERFORMING ORGANIZATION NAME AND ADDRESS The Aerospace Corporation El Segundo, California 90245	11. CONTROLLING OFFICE NAME AND ADDRESS Air Force Weapons Laboratory Kirtland Air Force Base, N. Mex. 87117	12. REPORT DATE 15 Aug 80
14. MONITORING AGENCY NAME & ADDRESS (if different from Controlling Office) Space Division Air Force Systems Command Los Angeles, Calif. 90009	13. NUMBER OF PAGES 52	15. SECURITY CLASS. (of this report) Unclassified
16. DISTRIBUTION STATEMENT (of this Report) Approved for public release; distribution unlimited.		
17. DISTRIBUTION STATEMENT (of the abstract entered in Block 20, if different from Report)		
18. SUPPLEMENTARY NOTES		
19. KEY WORDS (Continue on reverse side if necessary and identify by block number) Beam quality Polarization scrambling Transverse mode control Rear cone Flat feedback mirror		
20. ABSTRACT (Continue on reverse side if necessary and identify by block number) A repetitively pulsed CO ₂ laser facility was developed for testing annular resonators. The large-aperture device exhibits generally uniform gain over an annular region of 18-cm outer and 10-cm inner diameter. The half-symmetric unstable resonator with internal axicon (HSURIA) was tested at equivalent Fresnel numbers up to 4.5. This resonator design incorporates a W-axicon mirror beam compactor that transforms a cylindrical mode region into an annular mode region. Two HSURIA configurations were evaluated		

DD FORM 1473
(FACSIMILE)UNCLASSIFIED 409367
SECURITY CLASSIFICATION OF THIS PAGE (When Data Entered)

UNCLASSIFIED

SECURITY CLASSIFICATION OF THIS PAGE(When Data Entered)

(1) with a rear conical mirror and (2) with a rear flat mirror in the annular leg.

With the rear cone, the aligned resonator produced a predominantly higher-order azimuthal mode with an on-axis null in the far field. The output was strongly linearly polarized with the electric-field vector tangential to the optic axis in both the near and far fields. The higher-order tangentially polarized mode appears to be the result of a geometric polarization scrambling effect caused by the rear cone. The boundary conditions for the conical or W-axicon mirrors imply that the radial electric field has a 180-deg phase shift on reflection, whereas the tangential component is unchanged. Thus, a tangentially polarized mode is self-reproducing, but a linearly polarized mode is not.

In order to eliminate the polarization scrambling effect in the HSURIA, the rear cone was replaced with a rear flat mirror. The HSURIA with a rear flat produced a central spot in the far field that indicated an $l = 0$ mode with no spatial variations in polarization. Beam quality was measured in terms of the ratio n^2 of the theoretical (geometric mode) power transmitted through an aperture of the central lobe diameter to the observed power; n^2 values as low as 1.2 were obtained. The variation of beam quality with tilt of the rear flat indicated a factor of 2 degradation in n^2 for a 20- μ rad tilt, which is in good agreement with theory.

UNCLASSIFIED

SECURITY CLASSIFICATION OF THIS PAGE(When Data Entered)

PREFACE

The authors thank Mark Gerard of the Aerophysics Laboratory and Will Garber of the Electronics Research Laboratory, The Aerospace Corporation, for their support in the development of our experimental facility and the performance of the experiments. We are grateful for the support of the Air Force Weapons Laboratory, Major Plummer, Contracting Officer.

We also thank Dr. Harold Mirels of the Aerophysics Laboratory and Dr. Gregory C. Dente of the Air Force Weapons Laboratory for discussions helpful in the preparation of this document.

Accession For	
NTIS GRA&I	
DDC TAB	
Unannounced	
Justification	
By	
Distribution/	
Availability Codes	
Dist	Avail and/or special
A	

CONTENTS

PREFACE	1
I. INTRODUCTION	9
II. DESCRIPTION OF APPARATUS	13
A. Resonator Mirrors	13
B. Prealignment Technique	19
C. Beam Diagnostics	22
III. EXPERIMENTAL RESULTS	25
A. Higher Order Azimuthal Modes	25
B. Polarizing Elements	28
C. HSURLA with Rear Flat Mirror	32
IV. CONCLUSION	43
APPENDICES	
A. MODE IN RESONATOR WITH CONICAL ELEMENTS	47
B. CENTRAL SPOT PATTERN	51
C. EFFECT OF INTERCAVITY POLARIZER	55
D. COMPACT LEG EXPERIMENTS	57
REFERENCES	61

FIGURES

1.	HSURIA geometry with a rear flat mirror in the annular leg	10
2.	Radial zero-power-gain distribution of CO ₂ pulsed discharge on the P(20) transition.	14
3.	Photograph of closed-cycle CO ₂ laser test bed for annular resonators with optical table.	15
4.	HSURIA geometry with rear cone in the annular leg	16
5.	Interferometric technique for aligning the annular leg of the HSURIA with a rear cone	19
6.	Alignment interferogram for the annular leg of the HSURIA with a rear cone.	21
7.	Alignment interferogram for the annular leg of the HSURIA with a rear flat	21
8.	Beam-quality diagnostics	23
9.	Near- and far-field patterns produced by HSURIA with a rear cone and the gain in the annular leg	26
10.	Near- and far-field polarization characteristics corresponding to Fig. 9	27
11.	Geometric polarization scrambling effect produced by a linearly polarized input beam incident on the inner cone of a W-axicon mirror	29
12.	Technique for measuring the reflectivity of conical and W-axicon mirrors as a function of polarization angle	30
13.	Near- and far-field patterns produced by HSURIA with a rear flat and the gain in the annular leg	33
14.	Beam quality (power in the bucket) data corresponding to Fig. 13	35
15.	Effect of tilt of the rear flat mirror on beam quality for the HSURIA with a rear flat	37

FIGURES (Cont.)

16.	Effect of tilt of the convex mirror on beam quality for the HSURIA with a rear flat	38
17.	Effect of tilt of the convex mirror on the near- and far-field patterns for the HSURIA with a rear flat $\theta_c = 0$ and $74 \mu\text{rad}$	40
18.	Effect of tilt of the convex mirror on the near- and far-field patterns for the HSURIA with a rear flat $\theta_c = 145 \mu\text{rad}$ and $218 \mu\text{rad}$	41

TABLES

I.	HSURIA Cavity Parameters	17
II.	Reflectivity of Diamond-Turned Optics at $\lambda = 10.6 \mu\text{m}$	31

I. INTRODUCTION

Transverse mode control in an annular gain medium is a problem of current interest. The annular gain geometry is efficient from volumetric considerations and minimizes parasitic effects resulting from long gain lengths. For example, a radial flow nozzle geometry will efficiently generate an annular cw chemical laser gain region.

Recent experimental work with annular resonators¹⁻³ includes experiments with the half-symmetric unstable resonator with internal axicon (HSURIA) as discussed by Mumola et al.³ HSURIA experiments (with the gain in the compact leg) have also been performed by J. Hanlon and C. Huguley of the Air Force Weapons Laboratory.⁴ In the basic HSURIA geometry shown in Fig. 1 a flat feedback mirror in the annular leg of the resonator is used; the mirror can be replaced with either a corner reflector or a cone to reduce sensitivity to misalignment.

In this report, polarization effects in the HSURIA are considered, especially the geometry utilizing a rear cone. The test bed used consisted of an 18-cm-diameter, repetitively pulsed CO₂ laser, which differed from the HeXe laser testbed arrangement of Ref. 3. With the Ref. 3 arrangement, a small change in the cavity length could cause selection of a particular transverse mode, because the longitudinal mode spacing was comparable or larger than the Doppler gain width. With the arrangement used for this study, a length change did not affect the transverse mode structure because of the

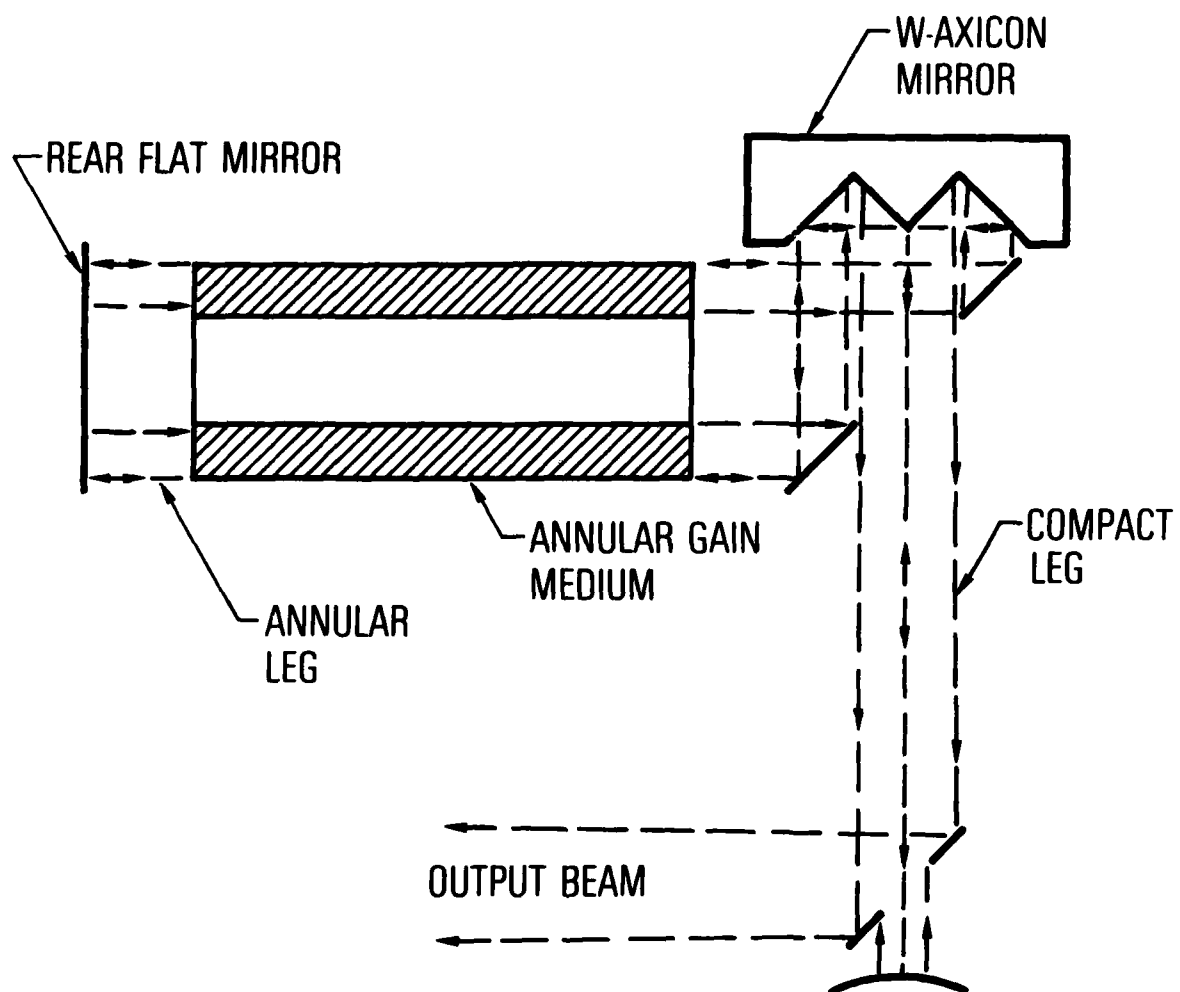


Fig. 1. HSURIA geometry with a rear flat mirror in the annular leg

long cavities and the number of available CO_2 transitions. The present HSURIA results also correspond to appreciably higher equivalent Fresnel numbers than those in Ref. 3 (up to $N_{\text{eq}} = 4.5$).

If an optical element in a resonator produces a polarizing, e.g., a Brewster window, effect for each round trip, the mode and polarization properties of the output radiation can be affected. For the conical aluminum mirrors used in these experiments, geometrical considerations⁶ and the mirror surface properties indicate that an azimuthal polarization is preferred over a linear polarization, which is consistent with a higher order azimuthal mode rather than the fundamental $l = 0$ mode. In this study, measurements were made of the near- and far-field polarization properties and the beam quality of the output from a HSURIA resonator incorporating both a rear cone and a flat feedback mirror in the annular leg; their characteristics were then compared. Performance with the gain in the annular leg was compared with that corresponding to the gain in the compact leg.

The work described herein was completed in January 1979.

II. DESCRIPTION OF APPARATUS

The test bed facility used in the CO_2 laser experiments is described in detail in Ref. 5. It consists of a repetitively pulsed CO_2 laser that uniformly excites a 0.94-m-long cylindrical gain region with an 18.7-cm-diameter clear aperture. The radial gain distribution, shown in Fig. 2 (from Ref. 5), indicates a peak zero-power gain of about 1.3 m^{-1} near the edge of the clear aperture of the ZnSe windows and about 0.9 m^{-1} on the centerline. The longitudinal flow, longitudinal discharge device operates at a repetition rate of 10 to 20 pulse/sec, peak current of 6 A, pulse width of 1 to 2 msec, pressure of 3 to 4 Torr, and $\text{CO}_2:\text{N}_2:\text{He}$ mixture of 1:1:4. A cw 60-mA glow discharge is superimposed on the pulse discharge to provide a uniform source of preionization. The voltage drop across the pulse discharge is typically 4 kV for the large bore 22-cm-diameter tube. The gas in the closed-cycle facility is circulated (1% makeup gas) by a 6500 cfm Roots pump with a compression ratio of approximately 4.6:1 at 4 Torr. The gas supply provides capacity for several hours continuous operation with a single filling. At pressures above about 4 Torr, arcing occurs in the discharge, and the medium homogeneity is severely degraded. Figure 3 is a photograph of the apparatus.

A. RESONATOR MIRRORS

The basic resonator evaluated consisted of the HSURLA with either a rear cone or a rear flat mirror. Figure 4 is the setup with the rear cone, and Table I is a list of the cavity parameters for the various geometries

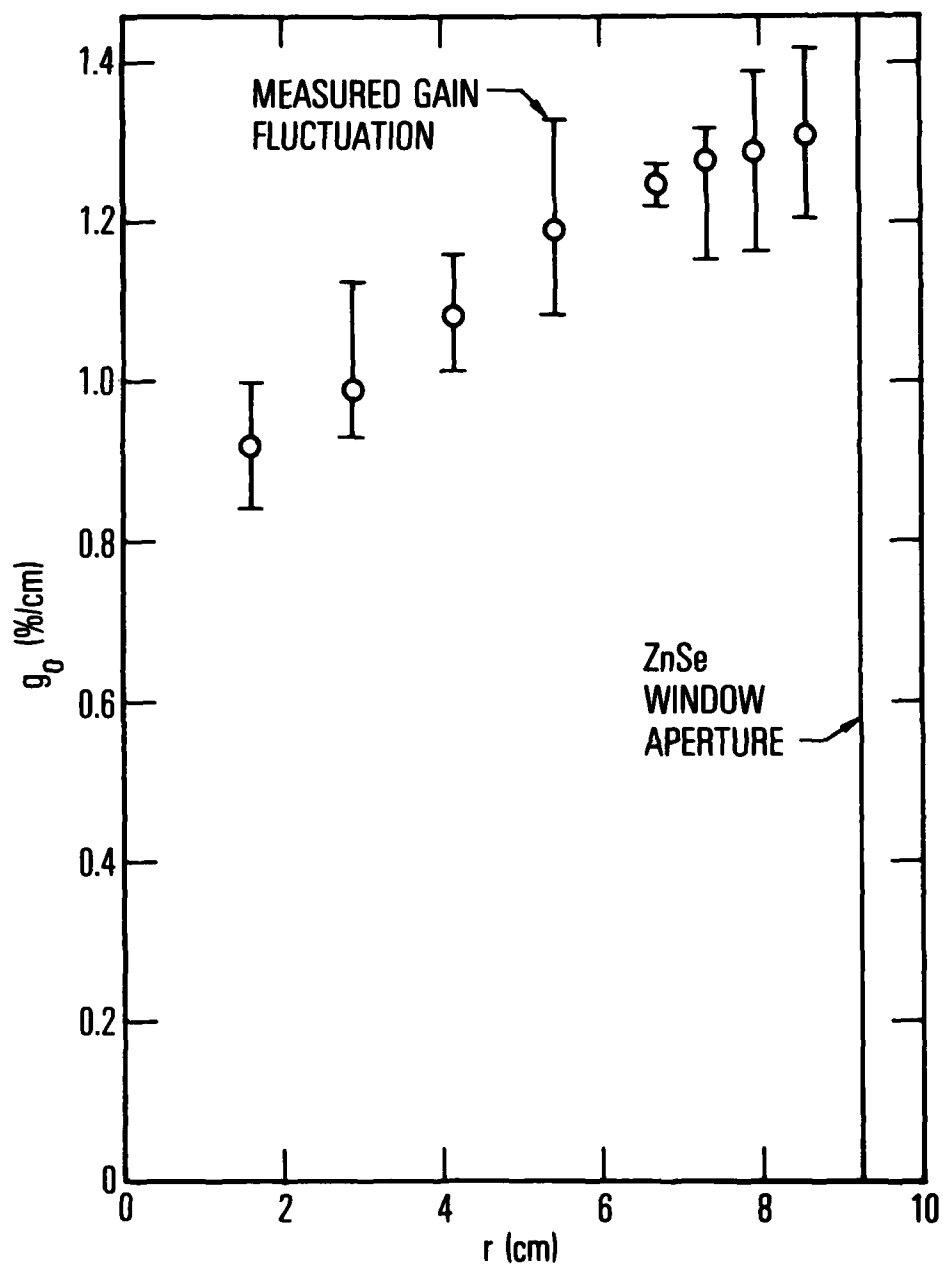


Fig. 2. Radial zero-power-gain distribution of CO_2 pulsed discharge on the P(20) transition

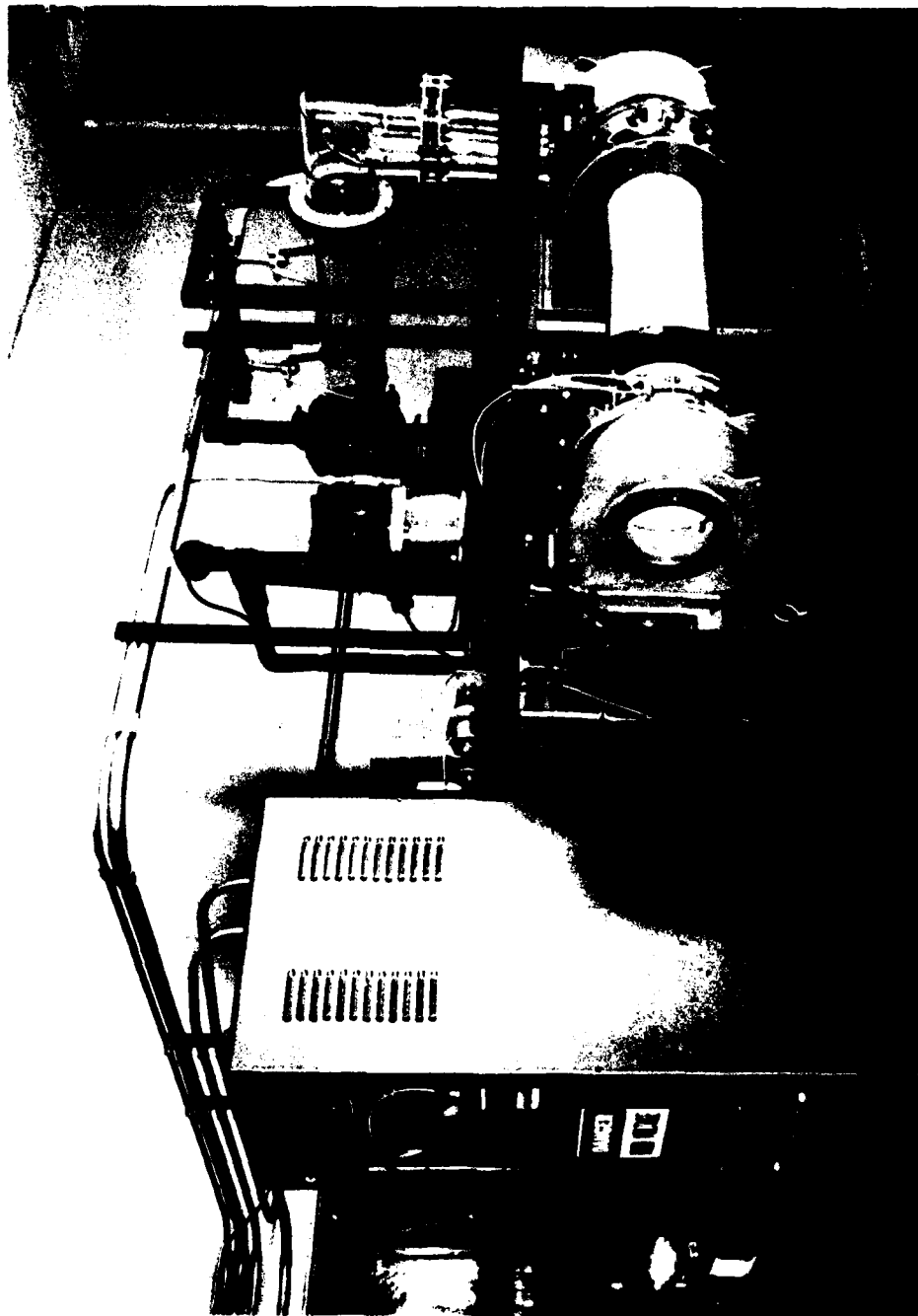


Fig. 3. Photograph of closed cycle CO_2 laser test bed for annular resonators with optical table

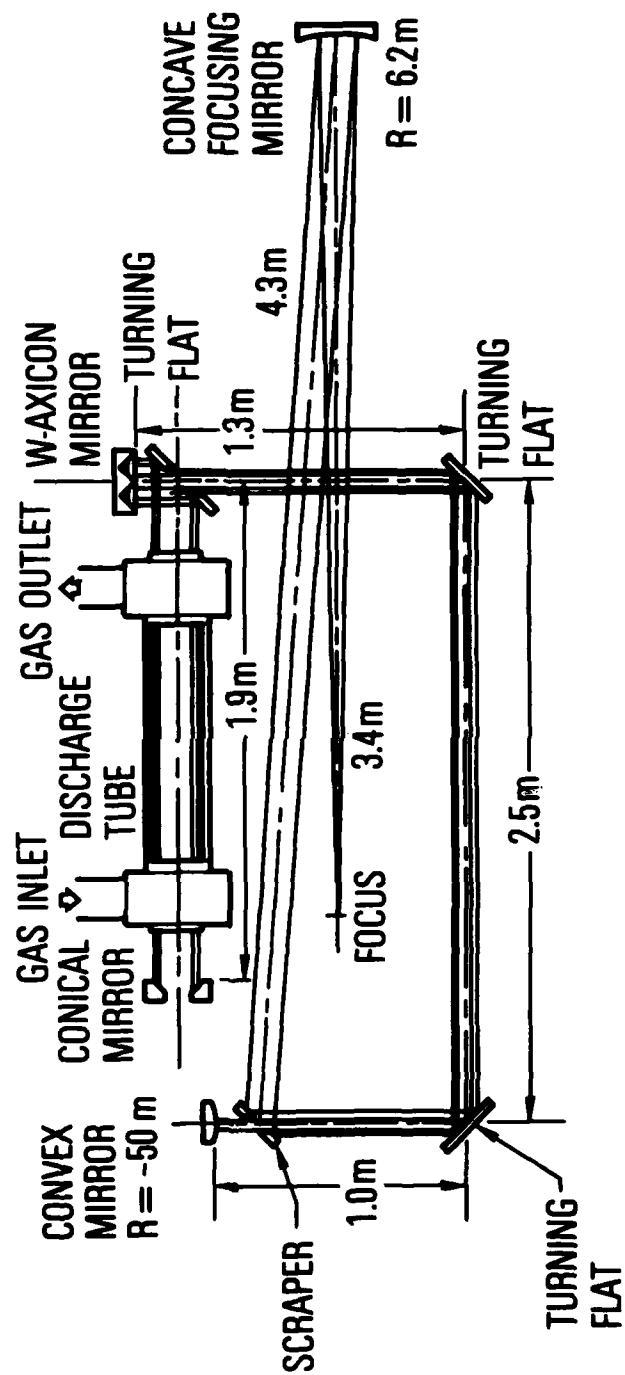


Fig. 4. HSURIA geometry with rear cone in the annular leg

Table I. HSURIA Cavity Parameters

Resonator	L, m	R, m	L _c , m	M	D _s , cm	N _{eq}
HSURIA/Rear Cone						
Gain in Annular Leg	7.1	-51.3	4.81	2.1	4.45	2.6
HSURIA/Rear Cone						
Gain in Compact Leg	3.47	-51.3	2.78	1.7	4.45	3.6
HSURIA/Rear Flat						
Gain in Annular Leg	3.36	-32.0	1.26	1.9	4.45	4.5

tested with the gain in either the annular or the compact leg. The parameters listed are cavity length L , radius of the convex mirror R , length of the compact leg L_c , magnification M , diameter of the small mirror D_s (determined by the position and hole diameter of the 45-deg output coupling mirror), and equivalent Fresnel number $N_{eq} = (D_s^2/4\lambda L)(M^2 - 1)/2M$. The compact leg experiments were conducted to allow comparison with previous results obtained at the AFWL by Hanlon and Huguley,⁴ who also used a rear cone in the annular leg.

The optical resonator was mounted on an NRC model RS-516-12 optical table, and the CO_2 gain cell was cantilevered over the table so optics were vibration-isolated. The diamond-turned W-axicon and cone were fabricated from aluminum at the Y-12 Union Carbide facility at Oak Ridge, Tennessee.

The dimension of the W-axicon mirror is determined by the position of the optic axis, which determines the outer dimension of the geometric mode in the annular leg. The outer diameters of the diamond-turned conical surfaces of both the W-axicon and the rear cone were 18.9 cm, and the optic axis diameter was 18.4 cm. The rear cone had a 9.5-cm diameter hole in the center, which permitted a maximum mode width of 4.7 cm in the annular leg. Both the W-axicon and the cone had flat, diamond-turned alignment surfaces machined perpendicular to the centerline near the outer edge. The W-axicon had a second flat alignment surface in the root region (5-mm wide) between the inner and outer cones. An interferogram was taken of the W-axicon, and an aberration of $0.95\text{ }\mu\text{m}$ was measured at $\lambda = 0.6328\text{ }\mu\text{m}$, which corresponds to $\lambda/11.0$ at $\lambda = 10.6\text{ }\mu\text{m}$.

Interferograms of the cone indicated an $8.3\text{-}\mu\text{rad}$ deviation from a 90-deg angle or a $1.58\text{-}\mu\text{m}$ optical path difference between the inner and outer edge. This is equivalent to a weak lens in the resonator of 8.5 km focal length and has little effect on performance. The two ZnSe windows, which were anti-reflection coated, had a mean single-pass aberration of $\lambda/16$ at $10.6\text{ }\mu\text{m}$ over the 18.7-cm-diameter clear aperture. The mirrors were fabricated from Pyrex and overcoated with gold, except for the convex mirrors which were fabricated from OHFC copper by Spawr Optical. The various mirror mounts used were manufactured by Aerotech Inc., Oriel, and the J. A. Noll Co.; they were attached to the optical table with magnetic bases.

B. PREALIGNMENT TECHNIQUE

The prealignment method is illustrated in Fig. 5. The annular leg was aligned with a Zygo interferometer, and the compact leg was aligned with alignment telescopes. The initial, annular leg alignment was accomplished by injecting a small-diameter HeNe beam along the optic axis onto the tip of the W-axicon. This generated a thin, 18.4-cm-diameter annular beam that defined the optic axis in the annular leg. The W-axicon could then be aligned with respect to the electric-discharge tube (with the windows removed), and the cone or flat could be roughly aligned by observing the return HeNe back at the source position. The circular return beam had a hole in the center that was a result of tip diffraction effects, and when the hole was at its minimum diameter, the annular leg was roughly aligned.

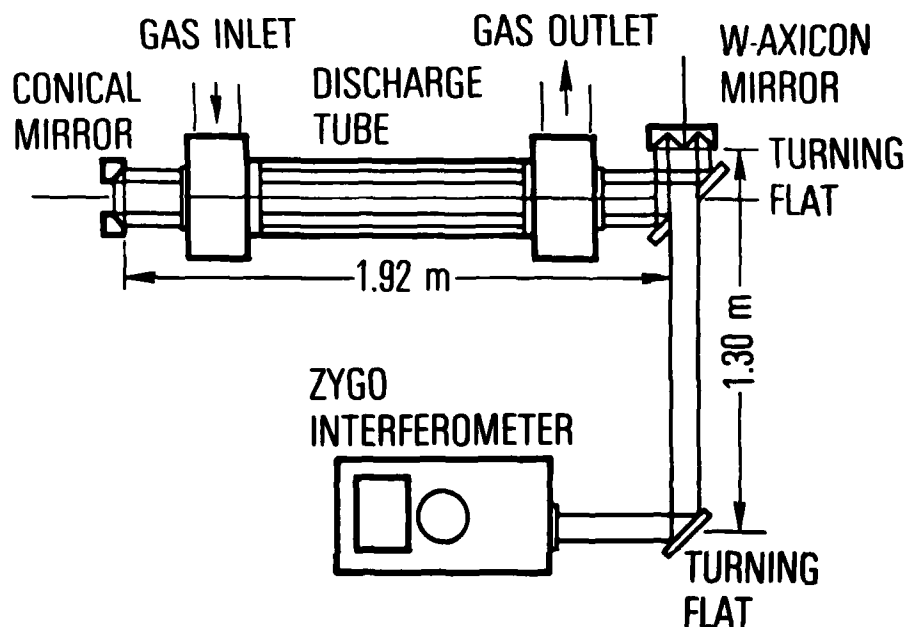


Fig. 5. Interferometric technique for aligning the annular leg of the HSURIA with a rear cone

The output beam from the Zygo interferometer was then inserted along the optic axis as indicated in Fig. 5 and aligned with respect to the fixed W-axicon when a null fringe off the flat alignment surface in the region of the root was obtained. For this interferometric prealignment to be precise, it was necessary to adjust the collimation of the Zygo beam by use of a shearing interferometer. After alignment of the Zygo with respect to the W-axicon, the rear cone (or flat) was adjusted to obtain the best null fringe possible. The interferogram shown in Fig. 6 was obtained by tilt and translation. Thus, a prealignment corresponding to three circular fringes (concentric with the optic axis) at $0.632 \mu\text{m}$ was obtained with the ZnSe windows in place and gas flowing in the discharge tube at 4 Torr. There were small figure errors in the W-axicon, but partial compensation could be made by misaligning the rear cone about 3 mrad. With the rear flat in the annular leg, however, no compensation could be made, and the best interferogram obtained, shown in Fig. 7, corresponds to about three fringes of aberration (double pass) because of the W-axicon.

After the annular leg was interferometrically aligned, the compact leg was aligned with two Davidson Model D275 alignment telescopes. One telescope was aligned with respect to the annular leg by simultaneously autocollimating off the rear flat and focusing on the W-axicon tip. A second telescope was then aligned with respect to the first by means of a 45-deg turning flat. The convex mirror was aligned with respect to the second alignment telescope by retroreflection. The prealignment of the compact leg was clearly



Fig. 6. Alignment interferogram for the annular leg of the HSURIA with a rear cone



Fig. 7. Alignment interferogram for the annular leg of the HSURIA with a rear flat

less precise than the prealignment of the annular leg, for which the interferometric method was used. The accuracy of the alignment telescopes limits the compact leg prealignment to about $\pm 100 \mu\text{rad}$. The scraper mirror was also centered with respect to the optic axis during this operation. The experimenters measured the tilt angle variations from the prealigned orientations by viewing flat mirrors attached to the back of the convex or rear cone mirrors with the alignment telescopes (in autocollimation). The alignment telescopes were accurate to within about $30 \mu\text{rad}$ in tilt. For more precise measurements, such as misalignment of the rear flat, the Zygo interferometer was used to observe the fringe shift with tilt angle.

C. BEAM DIAGNOSTICS

The parameters measured in the present HSURIA experiments include output power, near-field intensity distribution, far-field intensity distribution, far-field power distribution (beam quality), power versus time, near-field polarization, and far-field polarization. Figure 8 is the diagnostic setup for measuring beam quality and viewing the far-field intensity distribution. The diverging output beam from the unstable cavity was focused with a 6.2-m radius concave mirror to a ZnSe 2-deg wedge beam splitter. The first surface-reflected component was directed to a multiple-hole aperture disk at the focal plane to provide the transmitted power, the second surface reflection provided the reference total power, and the transmitted beam went to a 21-mm focal length ZnSe negative lens, which magnified the focal spot about a factor of 10 onto an Optical Engineering ZnSe thermal image screen.

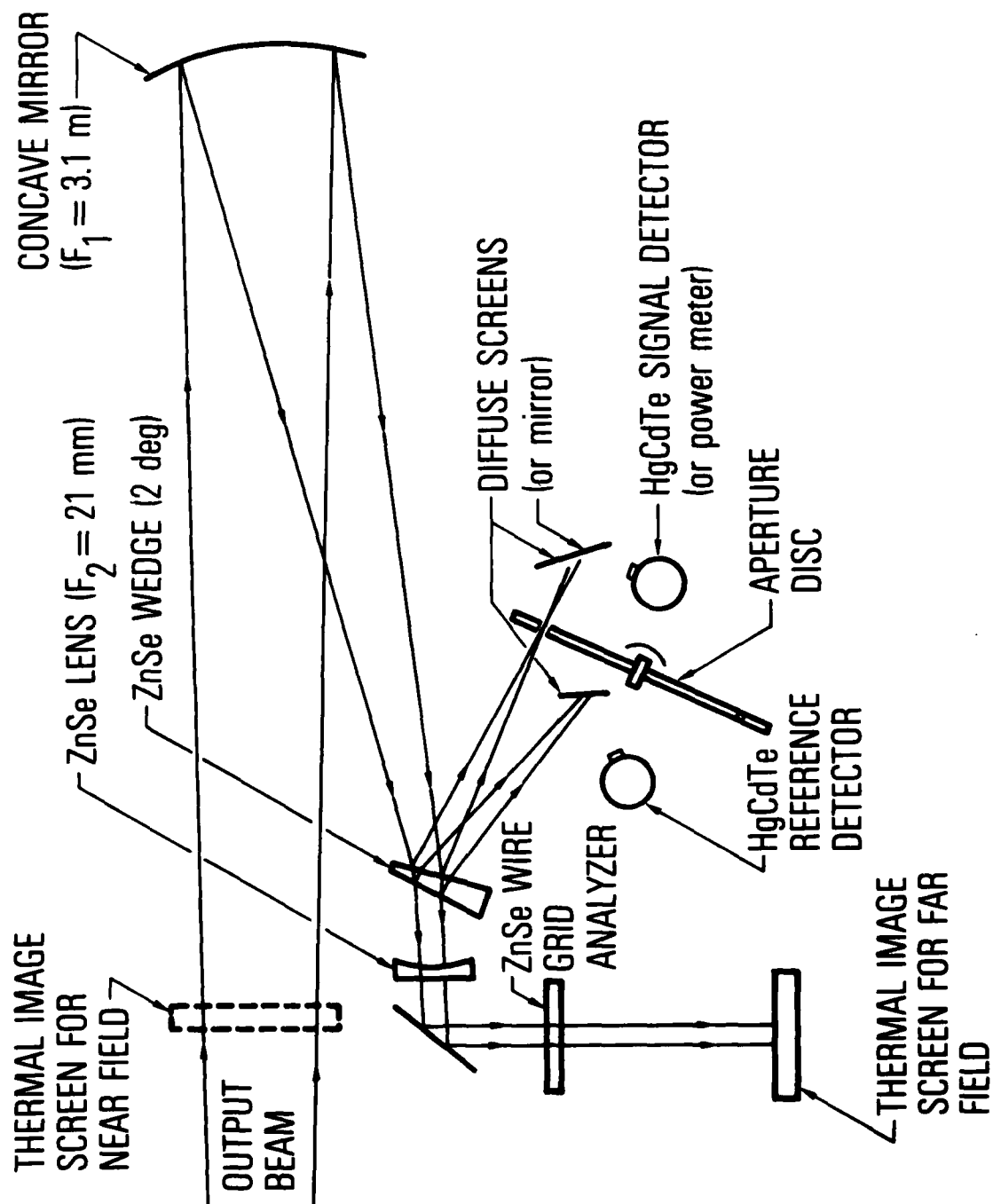


Fig. 8. Beam-quality diagnostics

Polarization effects were important in these experiments, and the angle of incidence on the beam splitter had to be kept small (~ 5 deg) to reduce the polarization sensitivity of the diagnostics. The power was measured by a CRL model 210 power meter or by Santa Barbara Research HgCdTe detectors viewing diffuse screens. The frequency bandwidth of the detectors was about 10 MHz. For measuring beam quality, the power transmitted was optimized through various diameter apertures mounted on Aerotech Model ATS-302 MMW remote-controlled xy translation stages. The fast detectors were used to measure the pulse-to-pulse variation in beam quality, as well as transverse mode beating phenomena.

The degree of linear polarization was measured with a 2-cm-diameter ZnSe wire grid analyzer manufactured by the PTR Corporation. The analyzer was placed between the lens and the thermal image screen to permit observation of the far-field polarization properties.

III. EXPERIMENTAL RESULTS

A. HIGHER ORDER AZIMUTHAL MODES

The HSURIA with a rear cone (gain in annular leg) shown in Fig. 4 (Table I) was prealigned as indicated by the interferogram in Fig. 6. The convex mirror was then tilted to produce the azimuthally uniform near-field pattern in Fig. 9, which also shows the corresponding far-field pattern. A convex mirror tilt correction of 100 to 200 μ rad was required; this is consistent with our compact leg prealignment accuracy. The far-field pattern shows an on-axis null. For an unstable resonator, the n th radial eigenmode can be expressed

$$u_n(r, \theta, z) = e^{-iAr^2} \sum_{l=-\infty}^{\infty} \psi_{nl}(r, z) e^{il\theta}$$

where l is the azimuthal mode number representing the angular mode dependence. For a given azimuthal mode number l , the $e^{il\theta}$ term represents a spiral wave front with a multi-valued phase at the origin. This implies a zero at the origin for any finite value of l ; therefore, only the $l = 0$ mode can have an intensity peak at the origin in the far field. The experimental far field in Fig. 9 thus corresponds to higher order azimuthal modes. The beam quality was measured by comparing the theoretical fractional power transmitted through an aperture of the diameter of the first null corresponding to the geometric magnification $M = 2.1$ (uniform phase) to the experimental value. This gave a value of

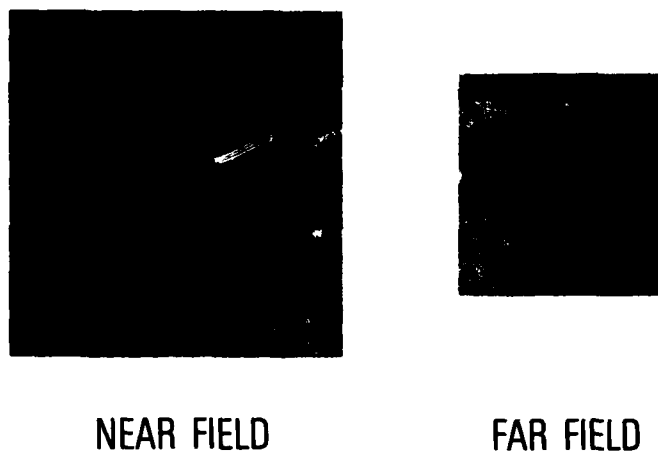


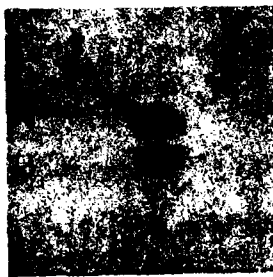
Fig. 9. Near-and far-field patterns produced by HSURIA with a rear cone and the gain in the annular leg (Table I). The convex mirror was tilted to produce an azimuthally uniform near field.

$P_{\text{theory}}/P_{\text{exp}} \equiv n^2 \approx 3.0$. The near- and far-field patterns in Fig. 9 were quite stable from pulse to pulse, and little high-frequency mode beating was observed.

A linear polarization analysis of the near- and far-field patterns in Fig. 9 is provided in Fig. 10. The mode patterns are azimuthally polarized in both the near and far fields. The degree of linear polarization in the near field was obtained by measuring the fraction of power transmitted through small holes in a mask at various azimuthal locations with the use of the wire grid analyzer. The degree of polarization was $\approx 50:1$.



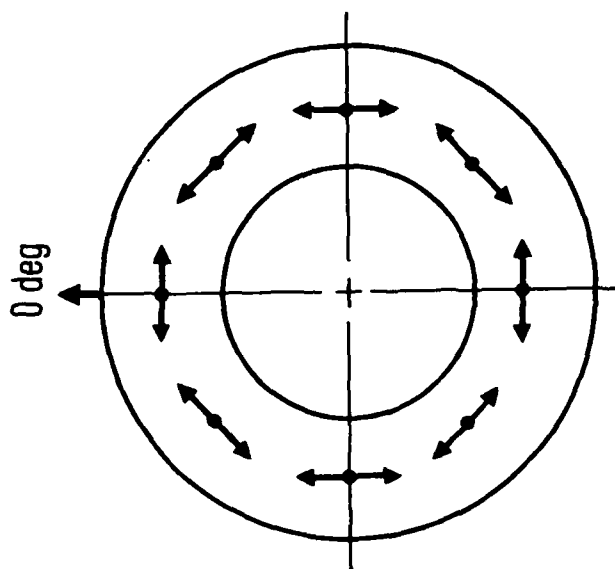
FAR-FIELD
PATTERN,
NO ANALYZER



VERTICAL
ANALYZER



HORIZONTAL
ANALYZER



NEAR-FIELD PATTERN, ARROWS
INDICATE DIRECTION OF POLARIZATION,
50:1 LINEAR POLARIZATION

Fig. 10. Near- and far-field polarization characteristics corresponding to Fig. 9. The far-field beam was transmitted through a wire grid linear analyzer.

B. POLARIZING ELEMENTS

The strong azimuthal polarization indicated the presence of a polarizing element within the resonator. Fink⁶ suggests that the strongest source of polarization selectivity is geometrical and is caused by the conical mirrors. The geometrical polarization scrambling effect caused by a W-axicon mirror for a linearly polarized input on the inner cone is shown in Fig. 11. A conical mirror produces a similar effect. Thus, on reflection, the radial component of the electric-field vector is rotated 180 deg, whereas the tangential component is unchanged. A tangentially polarized mode, therefore, would be self-reproducing on reflection off a W-axicon or a conical mirror. Polarization effects for an unstable resonator with a conical mirror, first investigated theoretically by Dente,⁷ are discussed in Appendix A. The experimental result of an azimuthally polarized higher order azimuthal mode ($l = 1$) for the HSURIA with a rear cone is consistent with this theory.

The surface properties of the diamond-turned aluminum cone or W-axicon can also produce polarization effects. A reflectivity experiment made with the aluminum cone and the W-axicon is shown in Fig. 12. Measurements for both the azimuthal and radial polarizations provided the single-surface reflectivity data shown in Table II. For the cone and W-axicon, 3.1% and 2.6% differences in reflectivity were measured between the azimuthal and radial polarizations, respectively. Corresponding measurements with two gold-coated flats made for comparison indicated no polarization effects. Because the rays strike six diamond-turned conical surfaces per round trip, this could be an additional strong selector for the azimuthally polarized mode.

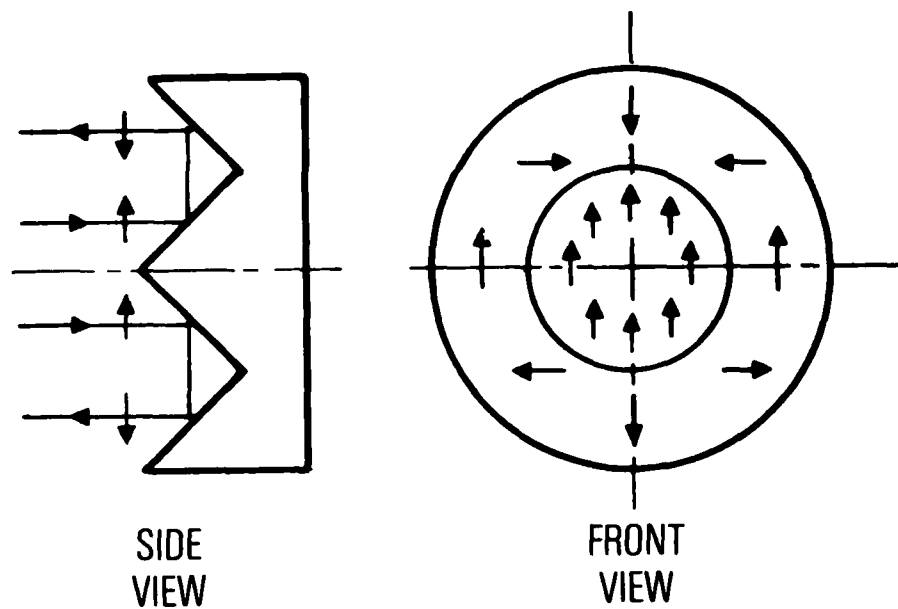


Fig. 11. Geometric polarization scrambling effect produced by a linearly polarized input beam incident on the inner cone of a W-axicon mirror. The radial electric field component is rotated 180 deg, and the tangential component is unchanged.

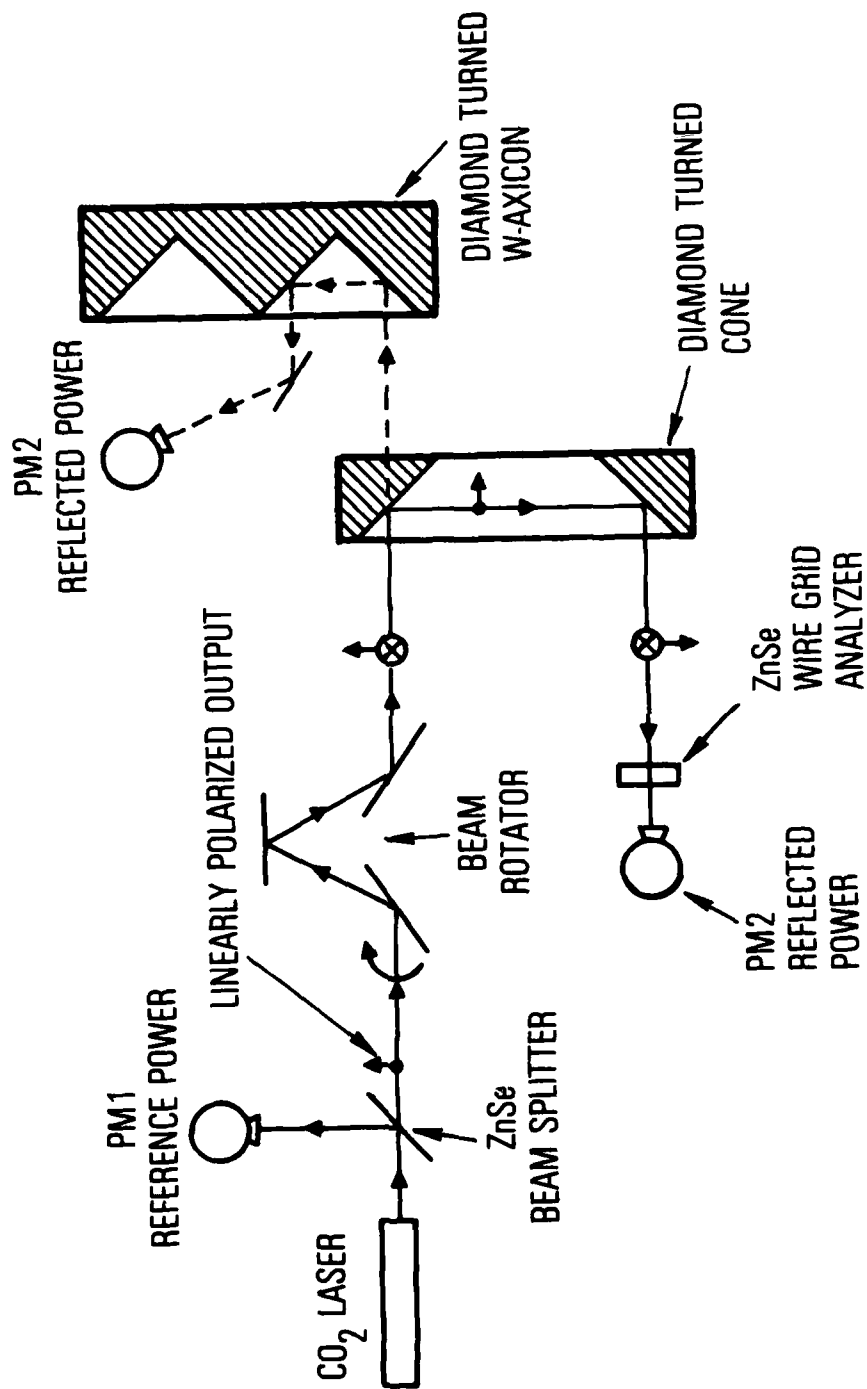


Fig. 12. Technique for measuring the reflectivity of conical and W-axicon mirrors as a function of polarization angle.

Table II. Reflectivity of Diamond-Turned Optics at $\lambda = 10.6 \mu\text{m}$

	Al Cone, %	Al W-Axicon, %	Au-Coated Glass, %
R_{\parallel}	95.1	95.1	97.9
R_{\perp}	98.2	97.7	97.9
Difference, %	3.1	2.6	0.0

The mechanism for the polarization-sensitive reflectivities has not been determined, but the diamond turning process might cause scattering in a direction defined by the machining.

Under certain conditions, a peak centerline intensity pattern can be obtained in the far field with the use of the HSURIA with the rear conical mirror. These far-field patterns correspond to a mixture of the $l = 0$ mode and higher order azimuthal components. For the case of the HSURIA with the gain in the annular leg, a central spot pattern can be obtained by misalignment of the convex mirror (see Appendix B). A similar result can be obtained if an intercavity polarizer is placed in the resonator to spoil the azimuthal polarization (Appendix C). For the case of the HSURIA with the gain in the compact leg, this central spot pattern was dominant, as discussed in Appendix D.

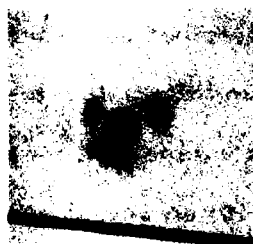
C. HSURIA WITH REAR FLAT MIRROR

The results shown in Figs. 9, 10, and 11 and Appendix A indicate that the conical surfaces in the HSURIA are the cause of the $l = 1$ mode. There is an odd number of reflections off polarization scrambling elements,⁶ because the radiation strikes the W-axicon twice and the rear cone once per round trip. For an odd number of reflections off cones or W-axicons per round trip, the eigenmode of the resonator is consistent with azimuthal polarization. For an even number of reflections off cones or W-axicons, the polarization scrambling effect should cancel, and the $l = 0$ mode should dominate. A HSURIA with a flat mirror, therefore, should oscillate in the $l = 0$ mode. This conclusion does not allow for surface polarization effects on the diamond-turned W-axicon, which could also cause selection of an azimuthal polarization based on the measurements (Table II). It was, therefore, of interest to measure the mode properties of the HSURIA with a rear flat.

Figure 13 shows the near- and far-field patterns obtained with the HSURIA with a rear flat mirror (Table I). This resonator is very sensitive to misalignment in comparison with the HSURIA with the rear cone, and the technique for obtaining single mode output differed. The resonator was initially prealigned. The gain medium was then activated, but the output was such that tilting the convex mirror alone could not produce an annular near-field or a diffraction-limited far-field spot. The rear flat mirror had to be tilted first to obtain an annular near-field output, and then the convex mirror tilted to obtain the optimum far-field pattern. After several repetitions of this procedure, the data in Fig. 13 were obtained.



NEAR FIELD PATTERN



FAR FIELD PATTERN

Fig. 13. Near-and far-field patterns produced by HSURIA with a rear flat and the gain in the annular leg (Table I)

The results indicate a well-defined far-field central spot with side lobes and an approximately uniform near-field annulus. The far-field pattern would remain stable for a few minutes, then the rear flat would have to be readjusted. There was also evidence of jitter in the central spot with the mirrors aligned. The instabilities in the far field are believed to be related to lack of stability in the mirror mounts in the annular leg. The far-field pattern had no variation on rotation of the linear analyzer, so the radiation was not azimuthally polarized. The polarization properties of the diamond-turned W-axicon do not seem to significantly affect the mode properties. The loss difference of approximately 10% (four reflections) per round trip between the azimuthal and radial polarizations is comparable to the calculated mode loss discrimination of the empty resonator.⁸ The measured transverse gain variation in Fig. 2 should, however, further enhance the transverse mode selectivity.⁹

The beam-quality data for the HSURIA with a rear flat are shown in Fig. 14. The far-field power distribution indicates a beam quality of $n^2 = 1.4$ based on the power meter, and the pulse-to-pulse variations made with the HgCdTe detectors gave peak values of $n^2 = 1.2$. These results are consistent with the beam jittering with an actual beam quality of $n^2 = 1.2$. This excellent beam quality indicates that the resonator is operating predominately in the $l = 0$ mode. An azimuthally uniform annulus could not be obtained, probably because of the aberrations in the W-axicon shown in Fig. 7.

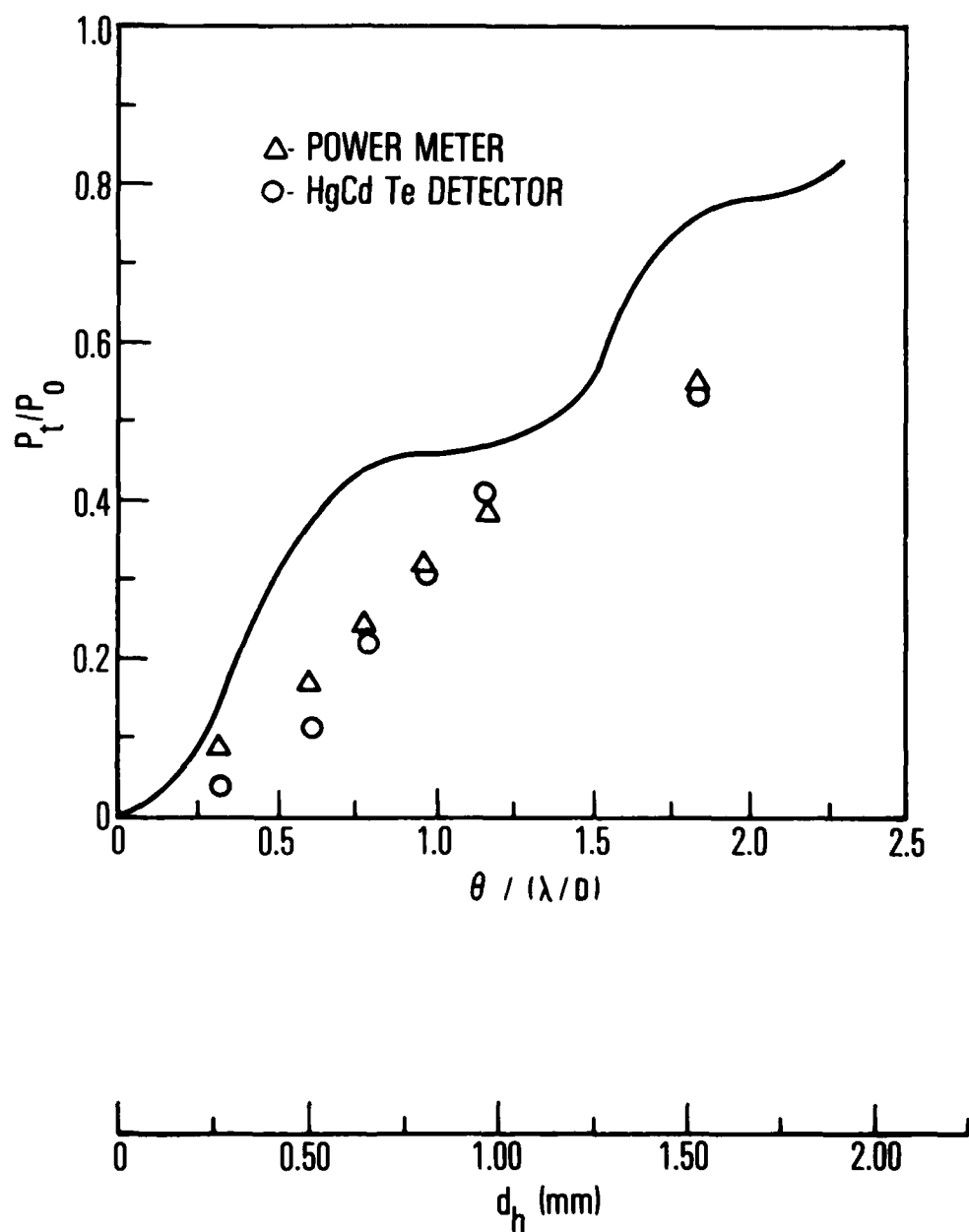


Fig. 14. Beam-quality (power in the bucket) data corresponding to Fig. 13. The theoretical power distribution for a uniformly illuminated annulus of constant phase and a geometric magnification of 1.9 is shown to allow comparison.

The misalignment sensitivity of the beam quality to tilt of the rear flat is shown in Fig. 15. The results were obtained by first aligning the rear flat for optimum beam quality (maximum power through an aperture of a fixed diameter corresponding to the first null), then tilting the flat in steps and optimizing the transmitted power for each step. The results indicate a reduction in beam quality (n^2) of a factor of 2 for a 20- μ rad misalignment of the rear flat. The radial motion of the optic axis off the tip of the W-axicon for a 20- μ rad tilt is about 0.1 mm, which is a small fraction of a Fresnel zone diameter (7 mm) based on the compact length of the resonator. A theoretical calculation⁸ made with the use of a three-dimensional, diffractive, empty cavity computer model, also shown in Fig. 15, exhibits good agreement for tilt angles up to 16 μ rad.

The misalignment sensitivity of the beam quality (n^2) to tilt of the convex mirror is shown in Fig. 16. The beam quality is much less sensitive to misalignment of the convex mirror, and a 300- μ rad tilt is required to reduce n^2 by a factor of 2. Tilting the convex mirror in a conventional half-symmetric unstable cavity displaces the optic axis. The amount of displacement for a 300- μ rad tilt is about 9 mm, or more than one Fresnel zone. It is surprising that the optic axis can be moved this far off the W-axicon tip without significantly degrading the beam quality. The theory in Ref. 8 was also compared to the experimental data in Fig. 16. The numerical method breaks down at about 75 μ rad, perhaps because the effect of gain was not considered. The near- and far-field patterns for different convex mirror tilt angles,

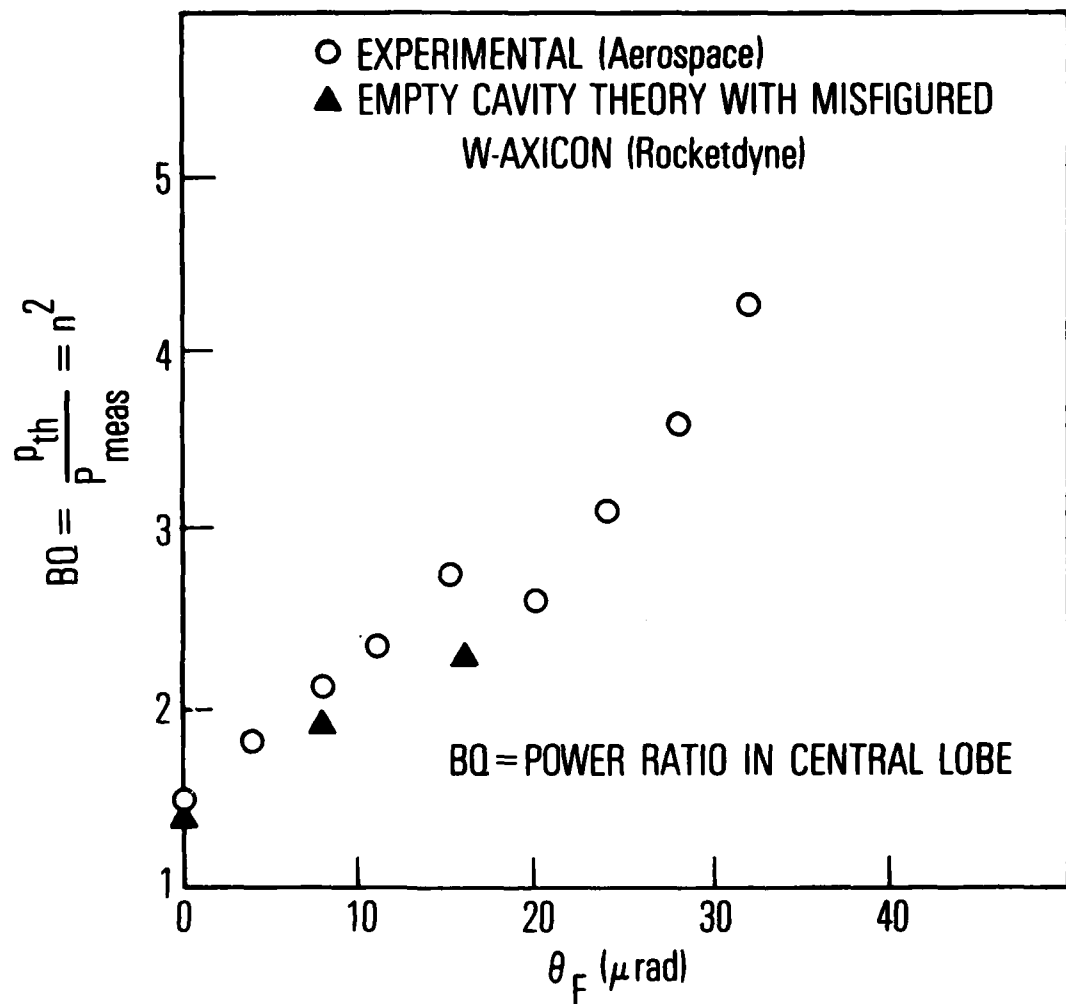


Fig. 15. Effect of tilt of the rear flat mirror on beam quality for the HSURIA with a rear flat (Fig. 13)

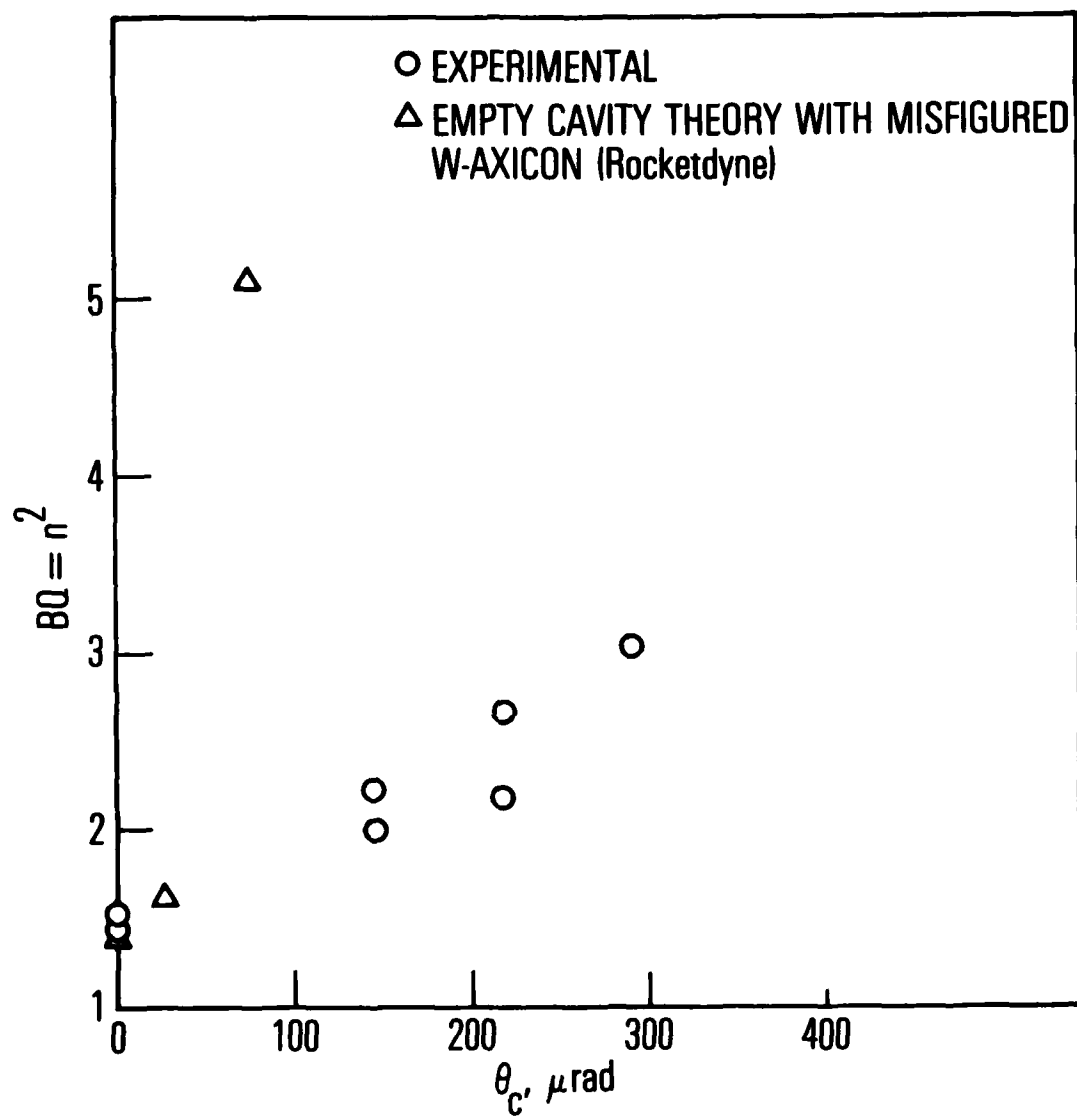
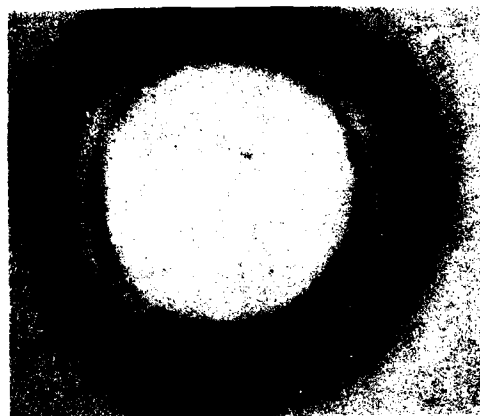


Fig. 16. Effect of tilt of the convex mirror on beam quality for the HSURIA with a rear flat (Fig. 13)

shown in Figs. 17 and 18, are consistent with a significant displacement of the optic axis, similar to that observed in a conventional half-symmetric unstable cavity.



NEAR FIELD

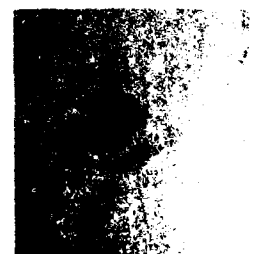


FAR FIELD

$$\theta_c = 0$$



NEAR FIELD



FAR FIELD

$$\theta_c = 73 \mu \text{rad}$$

Fig. 17. Effect of tilt of the convex mirror on the near-and far-field patterns for the HSURIA with a rear flat (Fig. 13) $\theta_c = 0$ and $74 \mu \text{rad}$

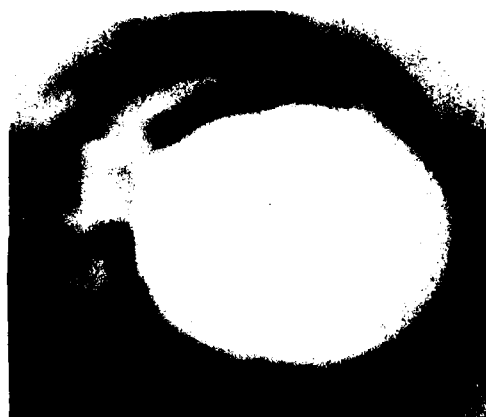


NEAR FIELD



FAR FIELD

$$\theta_c = 145 \mu\text{rad}$$



NEAR FIELD



FAR FIELD

$$\theta_c = 218 \mu\text{rad}$$

Fig. 18. Effect of tilt of the convex mirror on the near-and far-field patterns for the HSURIA with a rear flat (Fig. 13) $\theta_c = 145 \mu\text{rad}$ and $218 \mu\text{rad}$

IV. CONCLUSION

A new repetitively pulsed CO_2 laser test facility for studying large Fresnel number annular resonators has been developed. The half-symmetric unstable resonator with internal axicon (HSURIA) has been studied in two configurations, with either a rear cone in the annular leg or a rear flat mirror at equivalent Fresnel numbers up to 4.5. For the gain region in the annular leg of the HSURIA with a rear cone, a doughnut (suggesting an $l = 1$) mode was observed that was strongly azimuthally polarized in both the near and far fields. The beam quality (based on the fraction of power transmitted through a hole of the diameter of the central lobe and the geometric theory) for this doughnut mode was $n^2 \simeq 3$. The source of this azimuthal polarization and the $l = 1$ mode appears to be a geometric scrambling effect caused by the rear cone as suggested by Fink.⁶ This scrambling effect results from an azimuthally dependent rotation of the electric field vector for a linearly polarized input beam incident on a conical mirror.

When the rear cone was replaced by a rear flat mirror, a central spot pattern (suggesting an $l = 0$ mode) with side lobes was observed in the far field. For the HSURIA with a rear flat, the polarization scrambling effect is essentially cancelled due to two reflections off the W-axicon mirror per round trip. The beam quality of this $l = 0$ mode was measured as high as $n^2 = 1.2$ during a single pulse. These data indicate that polarization effects must be considered in the design of a HSURIA and should be incorporated into

mathematical models that formerly were based on scalar diffraction theory. Dente⁷ has developed an asymptotic diffraction theory for a half-symmetric unstable resonator with a conical mirror that considers the polarization scrambling effect (Appendix A). This theory predicts many of the experimental results.

Further testing of the HSURIA with the rear cone showed a temporarily unstable central spot mode (Appendix B) in the far field in addition to the stable $l = 1$ mode. The beam quality of this central spot mode was as high as $n^2 = 1.5$ during a single pulse, but it would stay in this mode for only a few minutes. The instability indicates strong transverse mode competition effects in this resonator which require further theoretical study. When the gain was placed in the compact leg of the HSURIA with the rear cone (Appendix D), a more stable central spot mode was obtained in the far field, but the beam quality was rather poor with $n^2 \simeq 2.5$. Strong transverse mode beating was observed in this configuration with beat frequencies ranging from 100 kHz to a few megahertz, again indicating mode competition effects. The difference between the compact leg and annular leg results is not yet understood.

Further tests of the HSURIA with the rear flat were made to measure the variation of beam quality with tilt of the rear flat and convex mirrors. The results indicate that the beam quality is very sensitive to misalignment of the rear flat with a 20- μ rad tilt sufficient to degrade n^2 by a factor of 2. The convex mirror had much less effect, with a 300- μ rad tilt reducing n^2 by a factor of 2. A 300- μ rad tilt of the convex mirror corresponds to a parallel

displacement of the optic axis of ≈ 9 mm, or about a Fresnel zone, and indicates that alignment of the optical axis with W-axicon tip is not required for good beam quality. The misalignment sensitivity of the rear flat can be reduced by replacing the flat with a rear corner cube as discussed in Ref. 3. For a hollow metal corner cube of high reflectivity, there are no polarization scrambling effects as observed with a rear cone.

APPENDIX A

Modes In Resonators With Conical Elements

The experimental results described in this paper provided some of the first evidence of the inadequacy of scalar resonator theory when applied to resonators with conical elements. In response to these data, a new theory was developed by Dente.^{7,10}

Standard resonator analysis, in which a linearly polarized mode is assumed, is inappropriate when the resonator contains conical elements. Therefore, we must proceed in a more general fashion. In the paraxial approximation, we can write an arbitrary electric field as a combination of azimuthal and radial polarizations, respectively. If we use a Jones Vector notation, this electric field takes the form

$$\begin{pmatrix} E_x \\ E_y \end{pmatrix} = f(r, \theta) \begin{pmatrix} \sin \theta \\ \cos \theta \end{pmatrix} + g(r, \theta) \begin{pmatrix} \sin \theta \\ -\cos \theta \end{pmatrix} \quad (A1)$$

in which our angle θ is measured counter-clockwise from the vertical (y) direction. If we perform a Fourier decomposition on $f(r, \theta)$, then

$$\begin{aligned} \begin{pmatrix} E_x \\ E_y \end{pmatrix} &= \sum_L f_L(r) e^{iL\theta} \begin{pmatrix} \cos \theta \\ \sin \theta \end{pmatrix} + \sum_L g_L(r) e^{iL\theta} \begin{pmatrix} \sin \theta \\ -\cos \theta \end{pmatrix} \\ &= \sum_L D_L(r) e^{i(L+1)\theta} \begin{pmatrix} 1 \\ -i \end{pmatrix} + \sum_L S_L(r) e^{i(L-1)\theta} \begin{pmatrix} 1 \\ i \end{pmatrix} \end{aligned} \quad (A2)$$

in which $D_L = f_L - ig_L$ and $S_L = f_L + ig_L$.

PRECEDING PAGE BLANK-NOT FILMED

The above vector decomposition of the fields was used by Dente^{7, 10} to obtain an empty cavity solution for a half symmetric unstable resonator with a conical mirror replacing the flat mirror. He made the calculation assuming the values of N_{eq} and M given in Table I corresponding to the HSURIA with the rear cone. Many of the experimental results obtained in this report were predicted by the theory.

It was found that the dominant mode ($L = 0$) is of the form

$$\begin{pmatrix} E_x \\ E_y \end{pmatrix} = f_0(r) \begin{pmatrix} \cos \theta \\ \sin \theta \end{pmatrix}$$

This mode has an azimuthally polarized near field, and an azimuthally polarized far field with an $\ell = 1$ intensity pattern, i.e., an on-axis null in the far field.

The analysis shows another higher order mode ($L = 1$) of the form

$$\begin{pmatrix} E_x \\ E_y \end{pmatrix} = f_1(r) e^{i\theta} \begin{pmatrix} \cos \theta \\ \sin \theta \end{pmatrix} \quad (A3)$$

$$= \frac{f_1(r)}{2} e^{2i\theta} \begin{pmatrix} 1 \\ -i \end{pmatrix} + \frac{f_1(r)}{2} \begin{pmatrix} 1 \\ i \end{pmatrix} \quad (A4)$$

Eq. (A3) shows an azimuthally polarized near-field intensity distribution that can be resolved into two components (Eq. (A4)). The far-field intensity distribution is obtained by taking the Fourier transform of Eq. (A4). The first term of the far field is proportional to $e^{2i\theta}$ and corresponds to an $\ell = 2$ azimuthal mode that will have an on-axis null. The second term has a uniform phase distribution and will have an on-axis peak corresponding to an $\ell = 0$ mode. The $\ell = 0$ portion will be right circularly polarized. The higher loss $L = 1$ mode hence is a linear combination of an $\ell = 0$ mode and an $\ell = 2$ mode, which is in qualitative agreement with the experimental results

in Fig. B1. The eigenvalue calculations indicated several closely spaced modes in the vicinity of the $L = 1$ mode which could cause the high-frequency mode beating observed.

APPENDIX B

Central Spot Pattern

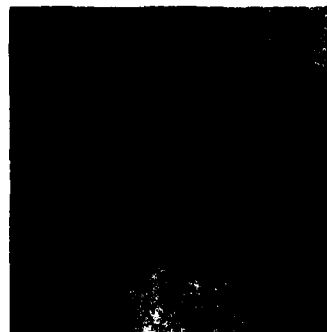
When the convex mirror was tilted to obtain the higher order azimuthal mode in Fig. 9, the far field occasionally changed spontaneously into a mode with an on-axis peak intensity, i. e., it had an $l = 0$ component. This far-field pattern was very unstable and sensitive to mirror tilt. With approximately 50 μ rad of tilt from the alignment of Fig. 9, the central spot pattern would appear and remain stable enough to obtain the near- and far-field data shown in Fig. B1. The output power of the resonator was measured for both the central spot and higher order mode operation and found to be identical to within 5% (10.5 W and 11.0 W, respectively). The near-field pattern corresponding to the central spot pattern in Fig. B1 is distinct from the higher order mode near-field pattern in Fig. 9. The far-field polarization measurements indicate that the central spot is linearly polarized, but the side lobe is azimuthally polarized. This is consistent with a combination of $l = 0$ and higher order azimuthal modes.

Beam-quality measurements of the central spot pattern in Fig. B1 are shown in Fig. B2. The upper scope trace corresponds to total power and the lower trace to power transmitted through an aperture. In the upper photograph, it is shown that the beam quality changes rapidly in time, with point A corresponding to $n^2 = 2.0$ and point B corresponding to $n^2 = 1.5$. In the lower photograph, the total power breaking into high-frequency oscillations within the pulse is shown. These frequencies, which occur in a range from 100 kHz to a few megahertz, are much less than the longitudinal mode beat frequency of 25 MHz and are probably caused by higher order transverse mode beating. Thus, the central spot pattern is probably a combination of competing transverse modes and is unstable, although the beam quality is at times very good.

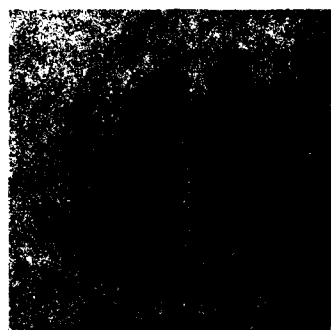
PRECEDING PAGE BLANK-NOT FILMED



NEAR FIELD



FAR FIELD,
NO ANALYZER



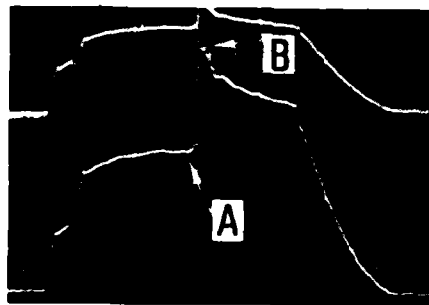
FAR FIELD,
VERTICAL ANALYZER



FAR FIELD,
HORIZONTAL ANALYZER

Fig. B1. Near-and far-field patterns produced by HSURIA with a rear cone and the gain in the annular leg (Table I). The convex mirror was tilted from the orientation corresponding to Fig. 9 approximately $50 \mu\text{rad}$ to obtain this central spot pattern.

POWER THROUGH 0.66-mm-diam
HOLE (central lobe)

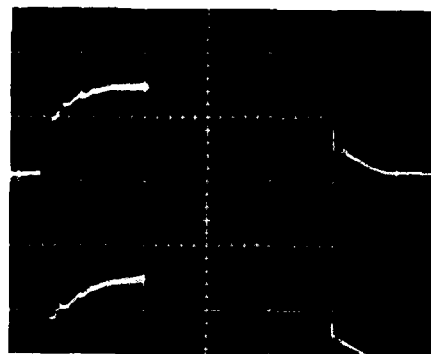


REFERENCE
DETECTOR

SIGNAL DETECTOR

$200\mu\text{sec/cm}$ diam

POWER THROUGH 1.27-cm-diam
HOLE (total power)



REFERENCE DETECTOR

SIGNAL DETECTOR

$200\mu\text{sec/cm}$ diam

Fig. B2. Beam-quality diagnostics corresponding to far-field patterns in Fig. B1. Total and transmitted power from HgCdTe detectors indicate rapid temporal variation in beam quality during laser pulse.

The central spot pattern observed is consistent with the theory set forth in Appendix A. The theory predicts two transverse modes (because of the polarization scrambling effect of the rear cone), a minimum loss $l = 1$ mode and a higher loss mixture of the $l = 0$ and $l = 2$ modes. Apparently, the higher loss mixture of the $l = 0$ and $l = 2$ modes can be obtained by misaligning the convex mirror, but it is less stable than the minimum loss $l = 1$ mode.

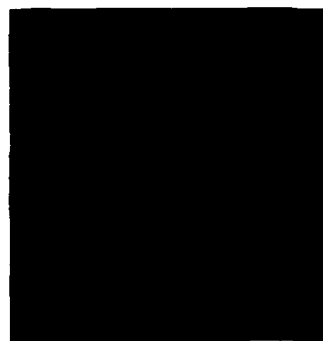
APPENDIX C

Effect of Intracavity Polarizer

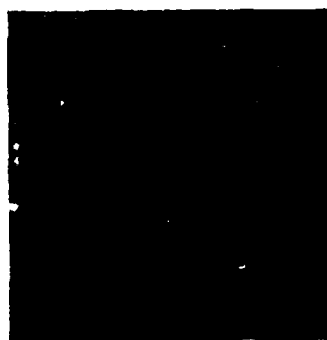
A NaCl Brewster window was placed inside the resonator between the scraper and convex mirrors. This provided an approximately 20% discrimination for linear polarization. The near- and far-field patterns obtained with the Brewster window in the cavity are shown in Fig. C1. The near field is not azimuthally uniform, possibly because of slight aberrations in the Brewster window. The far-field pattern, however, indicates a distinct (stable) central spot with side lobes. The central spot was linearly polarized in a direction consistent with the Brewster window orientation. The side lobe was not linearly polarized and corresponded to a higher order azimuthal mode. The beam quality was $n^2 \approx 2.0$. It appears that a linear intracavity polarizer can help discriminate against the $l = 1$ mode but cannot suppress all higher-order azimuthal modes.



NEAR FIELD



FAR FIELD,
NO ANALYZER



FAR FIELD,
VERTICAL ANALYZER



FAR FIELD,
HORIZONTAL ANALYZER

Fig. C1. Near-and far-field patterns produced by HSURIA with a rear cone, the gain in the annular leg, and an intercavity polarizer (Table I). The far-field beam was transmitted through a wire grid linear analyzer. Beam quality is $n^2 \approx 2.1$.

APPENDIX D

Compact-Leg Experiments

To permit comparison with results of Hanlon and Huguley⁴, experiments were made with the gain in the compact leg of the HSURIA as shown in Fig. D1 (Table I). The near - and far -field patterns obtained after an interferometric prealignment of the annular leg identical to that in Fig. 6 are shown in Fig. D2. The convex mirror was tilted to give the azimuthally uniform near field shown. The corresponding far -field pattern has a central spot in contrast to our results with the gain in the annular leg. The beam quality was $n^2 \approx 2.5$. Similar results were obtained in Ref. 4. The poor beam quality indicates that the output is not a pure $l = 0$ mode, and higher order azimuthal components may be present. Experiments demonstrated that the near -field polarization had both radial and azimuthal components, and the degree of polarization was less than the data in Fig. 10. The difference between the compact and annular leg results is not yet understood.

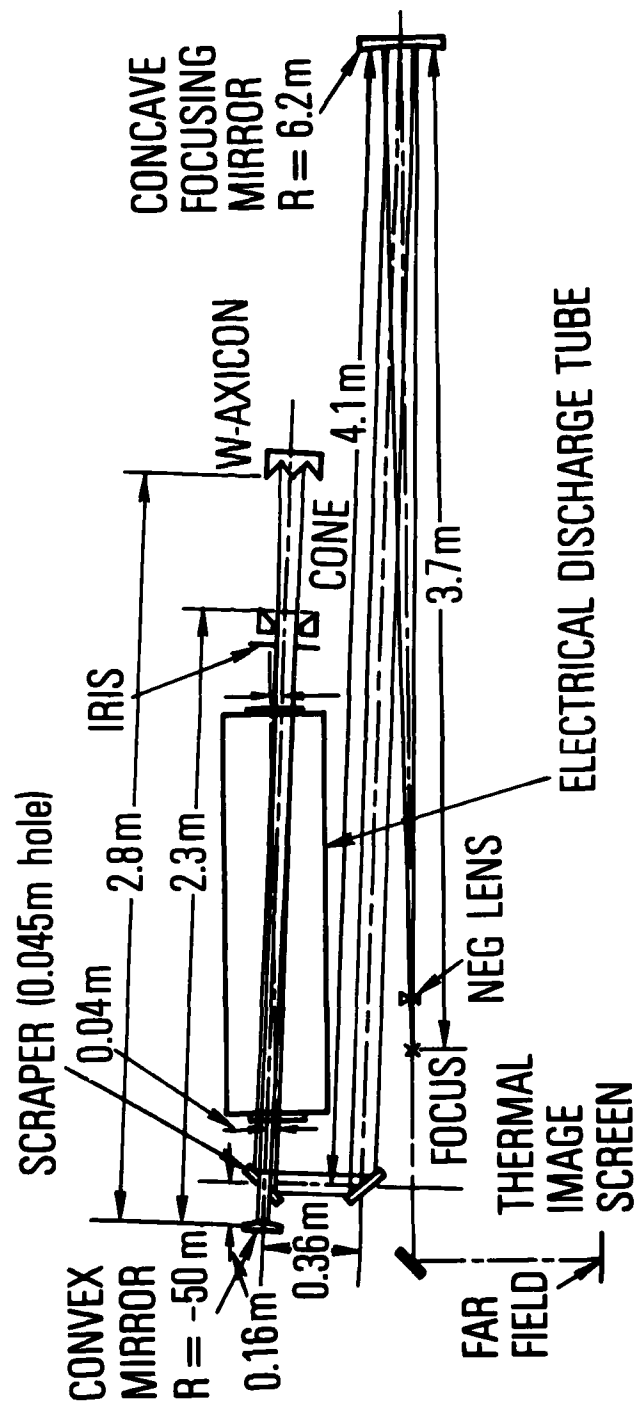


Fig. D1. HSURIA configuration with the gain in the compact leg



NEAR-FIELD PATTERN



FAR-FIELD PATTERN

Fig. D2. Near-and far-field patterns produced by HSURIA with a rear cone and the gain in the compact leg (Table I)

REFERENCES

1. L.W. Casperson and M.S. Shekhani, Appl. Opt. 14, 2653 (1975).
2. R.A. Chodzko, S.B. Mason, and E.F. Cross, Appl. Opt. 15, 2137 (1976).
3. P.B. Mumola, H.J. Robertson, G.N. Steinber, J.L. Kruezer, and A.W. McCullough, Appl. Opt. 17, 936 (1978).
4. J. Hanlon and C. Huguley, Air Force Weapons Laboratory, private communication.
5. E. B. Turner and R. A. Chodzko, Technical Report, The Aerospace Corporation (to be published).
6. D. Fink, Appl. Opt. 18, 581 (1979).
7. G. C. Dente, Appl. Opt. 18, 2911 (1979).
8. M. Bernabe, Rocketdyne Division of Rockwell International, Canoga Park, Calif., private communication.
9. J. W. Ellinwood, The Aerospace Corporation, private communication.
10. G. C. Dente, et al. Air Force Weapons Laboratory (unpublished).

LABORATORY OPERATIONS

The Laboratory Operations of The Aerospace Corporation is conducting experimental and theoretical investigations necessary for the evaluation and application of scientific advances to new military concepts and systems. Versatility and flexibility have been developed to a high degree by the laboratory personnel in dealing with the many problems encountered in the nation's rapidly developing space and missile systems. Expertise in the latest scientific developments is vital to the accomplishment of tasks related to these problems. The laboratories that contribute to this research are:

Aerophysics Laboratory: Launch and reentry aerodynamics, heat transfer, reentry physics, chemical kinetics, structural mechanics, flight dynamics, atmospheric pollution, and high-power gas lasers.

Chemistry and Physics Laboratory: Atmospheric reactions and atmospheric optics, chemical reactions in polluted atmospheres, chemical reactions of excited species in rocket plumes, chemical thermodynamics, plasma and laser-induced reactions, laser chemistry, propulsion chemistry, space vacuum and radiation effects on materials, lubrication and surface phenomena, photo-sensitive materials and sensors, high precision laser ranging, and the application of physics and chemistry to problems of law enforcement and biomedicine.

Electronics Research Laboratory: Electromagnetic theory, devices, and propagation phenomena, including plasma electromagnetics; quantum electronics, lasers, and electro-optics; communication sciences, applied electronics, semi-conducting, superconducting, and crystal device physics, optical and acoustical imaging; atmospheric pollution; millimeter wave and far-infrared technology.

Materials Sciences Laboratory: Development of new materials; metal matrix composites and new forms of carbon; test and evaluation of graphite and ceramics in reentry; spacecraft materials and electronic components in nuclear weapons environment; application of fracture mechanics to stress corrosion and fatigue-induced fractures in structural metals.

Space Sciences Laboratory: Atmospheric and ionospheric physics, radiation from the atmosphere, density and composition of the atmosphere, aurorae and airglow; magnetospheric physics, cosmic rays, generation and propagation of plasma waves in the magnetosphere; solar physics, studies of solar magnetic fields; space astronomy, x-ray astronomy; the effects of nuclear explosions, magnetic storms, and solar activity on the earth's atmosphere, ionosphere, and magnetosphere; the effects of optical, electromagnetic, and particulate radiations in space on space systems.

THE AEROSPACE CORPORATION
El Segundo, California